Information Sciences 180 (2010) 4641–4660

Contents lists available at ScienceDirect

Information Sciences

journal homepage: www.elsevier.com/locate/ins

MIMO adaptive fuzzy terminal sliding-mode controller for robotic manipulators

Tzuu-Hseng S. Li *, Yun-Cheng Huang

aiRobots Laboratory, Department of Electrical Engineering, National Cheng Kung University, Tainan 70101, Taiwan, ROC

ARTICLE INFO

Article history:
Received 26 August 2008
Received in revised form 23 July 2010
Accepted 7 August 2010

Keywords:
Adaptive control
Fuzzy logic controller
Robotic manipulators
Sliding-mode
Terminal sliding-mode

ABSTRACT

A new design approach of a multiple-input–multiple-output (MIMO) adaptive fuzzy terminal sliding-mode controller (AFTSMC) for robotic manipulators is described in this article. A terminal sliding-mode controller (TSMC) can drive system tracking error to converge to zero in finite time. The AFTSMC, incorporating the fuzzy logic controller (FLC), the TSMC, and an adaptive scheme, is designed to retain the advantages of the TSMC while reducing the chattering. The adaptive law is designed on the basis of the Lyapunov stability criterion. The self-tuning parameters are adapted online to improve the performance of the fuzzy terminal sliding-mode controller (FTSMC). Thus, it does not require detailed system parameters for the presented AFTSMC. The simulation results demonstrate that the MIMO AFTSMC can provide a reasonable tracking performance.

1. Introduction

It is well known that robotic manipulators have to encounter nonlinearities and various uncertainties in their dynamic models, such as friction, disturbance, and load changing, and it is very difficult to reach excellent performance when the control algorithm is completely based on the robotic plant model. Thus, designing a robotic manipulator controller is a serious challenge for engineers. In the last few decades, the sliding-mode control strategy has received special attention [3,8,10–12,14,17,18,20,24,37,45,46] because this method provides a systematic approach to retaining asymptotic stability and robust performance. However, chattering is a drawback of the sliding-mode control. While fuzzy logic has been applied to nonlinear systems with uncertainties [1,2,9,13,19,21,22,26–29,35,36,38,42,43,47,50,51], the large number of fuzzy rules makes the design complex.

Recently, the concept of integrating fuzzy logic control and sliding-mode control has become a popular research subject [3,8,10,11,17,18,20,24,37,45,46]. Fuzzy sliding-mode control can reduce the rule number in FLC, eliminate the chattering of sliding-mode control, and possess robustness in the presence of model uncertainty and disturbances. Hsu et al. [11] presented a fuzzy adaptive control law using the concept of variable structure, a control algorithm that does not require a system model. Guo and Woo [8] proposed an adaptive fuzzy sliding-mode control algorithm based on model information that is partially known. In [24], a T-S fuzzy-model-based SMC scheme is presented, and it does not assume that the control matrices of each T-S local linear model are identical. In [4,6,16,23,30,48], fuzzy neural networks are combined with the sliding-mode algorithm to control nonlinear systems. These controllers are used to reduce the chattering of the sliding-mode control and improve the tracking performance based on the system parameters that are partially known.

Another approach, called the terminal sliding-mode control, has been developed in [7,15,25,41,44,49,52,53]. Different from the classical sliding-mode, the terminal sliding-mode has a nonlinear sliding surface. While reaching the terminal

* Corresponding author. Tel.: +886 6 2757575; fax: +886 6 2345482.
E-mail address: thsli@mail.ncku.edu.tw (T-H.S. Li).

0020-0255/$ - see front matter © 2010 Elsevier Inc. All rights reserved.
doi:10.1016/j.ins.2010.08.009

sliding-mode, the system tracking error can be converged to zero in finite time. However, the system tracking error converges to zero asymptotically in the classical sliding-mode. That is, the system tracking error converges to zero in infinite time.

In this study, a new MIMO AFTSMC is proposed for robotic manipulators, which combines the MIMO FLC, the TSMC, and the adaptive scheme. The control algorithm is developed by combining the fuzzy method with the TSMC approach, which provides a simple way to design the fuzzy controller systematically and drives the system tracking error to converge to zero in finite time. The fuzzy terminal sliding-mode controller (FTSMC) can not only reduce the rule number in the FLC, but also reduce the chattering in the TSMC. The parameters of the normalization factor of output variable in the fuzzy mechanism and the output of the compensator are adapted online to improve the performance of the fuzzy terminal sliding-mode control system. The adaptive scheme does not require prior knowledge of dynamic parameters and can adjust the parameters of the controllers to reduce the error between the plant and the desired trajectories. This control algorithm can be applied to n-link robotic manipulators with unmodeled dynamics, unstructured uncertainties, and external disturbances. There are several advantages to the proposed control algorithm. First, it does not require system parameters. Second, the control input chattering is reduced. Third, the system tracking error converges to zero in finite time. Finally, the normalization factor of the output variable in the fuzzy mechanism and the output value of the compensator are adapted online.

This study is organized as follows. In Section 2, the TSMC for robotic manipulators is proposed. In Section 3, we propose a design method for MIMO AFTSMC for robotic manipulators. Section 4 gives the simulation example, and the conclusions are given in Section 5.

2. TSMC for robotic manipulators

This section describes the TSMC that is applied to robotic manipulators. The TSMC design can be decoupled in two steps. The first step is the selection of an appropriate terminal sliding surface. The second step, a discontinuous control law, is designed so that it will drive the system state toward terminal sliding surface and guarantee the stability of the system.

Consider the dynamic equation of general n-link robotic manipulators [40]

$$\mathbf{H}(\mathbf{q})\ddot{\mathbf{q}} + \mathbf{C}(\mathbf{q},\dot{\mathbf{q}})\dot{q} + \mathbf{G}(\mathbf{q}) + \mathbf{T}_d = \boldsymbol{\tau}, \tag{1}$$

where

$\mathbf{q} \in R^n$ is the joint angular position vector;
$\dot{\mathbf{q}} \in R^n$ is the joint angular velocity vector;
$\ddot{\mathbf{q}} \in R^n$ is the joint angular acceleration vector;
$\boldsymbol{\tau} \in R^n$ is the vector of the control input;
$\mathbf{H}(\mathbf{q}) \in R^{n\times n}$ is the inertia matrix;
$\mathbf{C}(\mathbf{q},\dot{\mathbf{q}}) \in R^{n\times n}$ is the matrix of Coriolis and centrifugal forces;
$\mathbf{G}(\mathbf{q}) \in R^n$ is the gravity vector; and
$\mathbf{T}_d \in R^n$ is the vector of generalized input due to disturbances or unmodeled dynamics.

The inertia matrix $\mathbf{H}(\mathbf{q})$ is symmetric and positive definite, and it is bounded as $m_1 \leqslant \|\mathbf{H}(\mathbf{q})\| \leqslant m_2$ where m_1 and m_2 are positive constants. The matrix $\dot{\mathbf{H}}(\mathbf{q}) - 2\mathbf{C}(\mathbf{q},\dot{\mathbf{q}})$ is a skew symmetric and satisfies $\mathbf{x}^T[\dot{\mathbf{H}}(\mathbf{q}) - 2\mathbf{C}(\mathbf{q},\dot{\mathbf{q}})]\mathbf{x} = 0$ where $\mathbf{x}$ is an $n \times 1$ nonzero vector. The gravity vector is bounded as $\|\mathbf{G}(\mathbf{q})\| \leqslant g_b$, where g_b is a positive function of $\mathbf{q}$. For simplification, $\mathbf{H}(\mathbf{q}), \mathbf{C}(\mathbf{q},\dot{\mathbf{q}})$, and $\mathbf{G}(\mathbf{q})$ are written as $\mathbf{H}$, $\mathbf{C}$, and $\mathbf{G}$, respectively.

Let the tracking error

$$\mathbf{e} = \mathbf{q} - \mathbf{q}_d, \tag{2}$$

where $\mathbf{q}$ is the joint position and $\mathbf{q}_d$ is the desired position.

To obtain the finite time convergence of the system tracking error, the terminal sliding surface is defined as

$$\mathbf{s} = \dot{\mathbf{e}} + \boldsymbol{\alpha}\mathbf{e}^{q/p}, \tag{3}$$

where $\boldsymbol{\alpha} = diag[\alpha_1,\ldots,\alpha_i,\ldots,\alpha_n]$ in which $\alpha_i\ (i = 1,\ldots,n)$ is a positive constant, p and q are positive odd integers and satisfy the following conditions [53],

$$p > q \quad \text{and} \quad 2q > p. \tag{4}$$

The terminal sliding-mode is then defined as $\mathbf{s} = \mathbf{0}$ or

$$\dot{\mathbf{e}} + \boldsymbol{\alpha}\mathbf{e}^{q/p} = 0. \tag{5}$$

Note that the control output of TSMC can be written as

$$\mathbf{u}(\mathbf{e},t) = \begin{cases} \mathbf{u}^{+}(\mathbf{e},t), & \text{when } \mathbf{s}(\mathbf{e}) > 0, \\ \mathbf{u}^{-}(\mathbf{e},t), & \text{when } \mathbf{s}(\mathbf{e}) < 0. \end{cases}$$

The terminal sliding surface **s** can be driven to the terminal sliding-mode **s** = **0** [53].

In the linear sliding-mode, the sliding surface is defined as

$$\mathbf{s} = \dot{\mathbf{e}} + \boldsymbol{\lambda}\mathbf{e}, \tag{6}$$

where $\boldsymbol{\lambda} = diag[\lambda_1, \ldots, \lambda_i, \ldots, \lambda_n]$ in which λ_i ($i = 1, \ldots, n$) is a positive constant. Then, the system tracking error converges to zero asymptotically.

However, in the terminal sliding-mode, the system tracking error can be expressed in the following form

$$\dot{e}_i = -\alpha_i e_i^{q/p}, \quad i = 1, \ldots, n. \tag{7}$$

The solution of Eq. (7) for the convergence time t_i ($i = 1, \ldots, n$) is given by

$$t_i = -\int_{e_i(0)}^{0} \frac{de_i}{\alpha_i e_i^{q/p}} = \frac{|e_i(0)|^{1-\frac{q}{p}}}{\alpha_i\left(1 - \frac{q}{p}\right)}, \tag{8}$$

where p and q are selected to satisfy (4); the initial value of e_i at $t = 0$ is $e_i(0)$. Thus, t_i is the convergence time of the tracking errors to zero after the terminal sliding-mode is attained.

We may interpret **s** of (3) as a "velocity error" term [39]

$$\mathbf{s} = \dot{\mathbf{e}} + \boldsymbol{\alpha}\mathbf{e}^{q/p} = \dot{\mathbf{q}} - \dot{\mathbf{q}}_\mathbf{d} + \boldsymbol{\alpha}\mathbf{e}^{q/p} = \dot{\mathbf{q}} - \dot{\mathbf{q}}_\mathbf{r}, \tag{9}$$

$$\dot{\mathbf{s}} = \ddot{\mathbf{e}} + \boldsymbol{\alpha}(\mathbf{e}^{q/p})' = \ddot{\mathbf{q}} - \ddot{\mathbf{q}}_\mathbf{d} + \boldsymbol{\alpha}(\mathbf{e}^{q/p})' = \ddot{\mathbf{q}} - \ddot{\mathbf{q}}_\mathbf{r}, \tag{10}$$

where

$$\dot{\mathbf{q}}_\mathbf{r} = \dot{\mathbf{q}}_\mathbf{d} - \boldsymbol{\alpha}\mathbf{e}^{q/p}, \tag{11}$$

$$\ddot{\mathbf{q}}_\mathbf{r} = \ddot{\mathbf{q}}_\mathbf{d} - \boldsymbol{\alpha}(\mathbf{e}^{q/p})'. \tag{12}$$

When the system is in the terminal sliding-mode, $\ddot{\mathbf{q}}_\mathbf{r}$ can be written as

$$\ddot{\mathbf{q}}_\mathbf{r} = \ddot{\mathbf{q}}_\mathbf{d} - \boldsymbol{\alpha}\frac{d}{dt}\left(\mathbf{e}^{q/p}\right) = \ddot{\mathbf{q}}_\mathbf{d} - \frac{q}{p} diag\left(\alpha_i e_i^{(q-p)/p}\right) \times \dot{\mathbf{e}} = \ddot{\mathbf{q}}_\mathbf{d} + \left[\alpha_1^2 \frac{q}{p} e_1^{(2q-p)/p}, \ldots, \alpha_i^2 \frac{q}{p} e_i^{(2q-p)/p}, \ldots, \alpha_n^2 \frac{q}{p} e_n^{(2q-p)/p}\right]^T, \tag{13}$$

where p and q satisfy $2q > p$, and then the vector $\ddot{\mathbf{q}}_\mathbf{r}$ should be bounded as the tracking error e_i converges to zero in the terminal sliding-mode.

Applying (9) and (10) into (1) leads to

$$\mathbf{H}\dot{\mathbf{s}} = \boldsymbol{\tau} - \mathbf{H}\ddot{\mathbf{q}}_r - \mathbf{C}\mathbf{s} - \mathbf{C}\dot{\mathbf{q}}_r - \mathbf{G} - \mathbf{T}_d. \tag{14}$$

To prove the stability of the system, we choose the Lyapunov function as

$$V = \frac{1}{2}\mathbf{s}^T\mathbf{H}\mathbf{s}. \tag{15}$$

The derivative of V becomes

$$\dot{V} = \mathbf{s}^T(\boldsymbol{\tau} - \mathbf{H}\ddot{\mathbf{q}}_r - \mathbf{C}\dot{\mathbf{q}}_r - \mathbf{G} - \mathbf{T}_d). \tag{16}$$

Choose the control input $\boldsymbol{\tau}$

$$\boldsymbol{\tau} = -\mathbf{K}sgn(\mathbf{s}), \tag{17}$$

where $\mathbf{K} = diag[K_{11}, \ldots, K_{ii}, \ldots, K_{nn}]$ is a diagonal positive definite matrix and K_{ii} ($i = 1, \ldots, n$) is a positive constant.

Substituting (17) into (16) yields

$$\dot{V} = \mathbf{s}^T[\mathbf{B} - \mathbf{K}sgn(\mathbf{s})] = \sum_{i=1}^{n} s_i[B_i - K_{ii}sgn(s_i)], \tag{18}$$

where

$$\mathbf{B} = -\mathbf{H}\ddot{\mathbf{q}}_r - \mathbf{C}\dot{\mathbf{q}}_r - \mathbf{G} - \mathbf{T}_d. \tag{19}$$

(a) When $s_i \neq 0$ and any $e_i \neq 0$.

From (13) and (19), it is easy to see that if **e** and $\dot{\mathbf{e}}$ are bounded, then **B** is bounded. Assuming $|B_i| < |B_i|^*$, where $|B_i|^*$ is the upper boundary of $|B_i|$. If **K** is chosen such that

$$K_{ii} > |B_i|^*, \tag{20}$$

this guarantees that the system tracking error is quickly convergent, and each K_{ii} should be chosen to be sufficiently large. When $s_i > 0$, from (20) we get

$$s_i[B_i - K_{ii}sgn(s_i)] < 0. \tag{21}$$

When $s_i < 0$, from (20) we get

$$s_i[B_i - K_{ii}sgn(s_i)] < 0. \tag{22}$$

Thus

$$\dot{V} = \sum_{i=1}^{n} s_i[B_i - K_{ii}sgn(s_i)] < 0. \tag{23}$$

(b) When system $s_i \neq 0$ and $e_i = 0$.
From (11), we obtain

$$\dot{\mathbf{q}}_\mathbf{r} = \dot{\mathbf{q}}_\mathbf{d} - \boldsymbol{\alpha}\mathbf{e}^{q/p} = \dot{\mathbf{q}}_\mathbf{d} - \left[\alpha_1 e_1^{q/p}, \ldots, \alpha_i e_i^{q/p}, \ldots, \alpha_n e_n^{q/p}\right]^T = \dot{\mathbf{q}}_\mathbf{d} - \left[\alpha_1 e_1^{q/p}, \ldots, 0, \ldots, \alpha_n e_n^{q/p}\right]^T. \tag{24}$$

From (12), we obtain

$$\ddot{\mathbf{q}}_\mathbf{r} = \ddot{\mathbf{q}}_\mathbf{d} - \boldsymbol{\alpha}\frac{d}{dt}\left(\mathbf{e}^{q/p}\right) = \left[\ddot{q}_{d1} - \alpha_1 \frac{q}{p} e_1^{(q-p)/p} \cdot \dot{e}_1, \ldots, \ddot{q}_{di} - \alpha_i \frac{q}{p} e_i^{(q-p)/p} \cdot \dot{e}_i, \ldots, \ddot{q}_{dn} - \alpha_n \frac{q}{p} e_n^{(q-p)/p} \cdot \dot{e}_n\right]^T, \tag{25}$$

where $\ddot{q}_{ri} = \ddot{q}_{di} - \alpha_i \frac{q}{p} e_i^{(q-p)/p} \cdot \dot{e}_i$.

In this case $s_i \neq 0$ and $e_i = 0, \ddot{q}_{ri}$ exists the singularity problem.

Refs. [44,53] addressed an approach to avoid the singularity. In the proposed method, singularity is avoided by switching from a terminal sliding surface to a general sliding surface. In this review, singularity is avoided by switching to a nonsingular terminal sliding surface (NTSS) [7]. The NTSS is described as follows:

$$s_i = \dot{e}_i^{p/q} + \alpha e_i, \tag{26}$$

where α, p and q have been defined in (3) and (13).

The derivative of s_i becomes

$$\dot{s}_i = \frac{p}{q} \dot{e}_i^{(p-q)/q} \cdot \ddot{e}_i + \alpha \dot{e}_i. \tag{27}$$

It can be seen that $\dot{s}_i$ does not result in negative powers. Thus, it is able to avoid the singularity problem.

Remark 1. In this article, singularity is avoided by switching, as follows:

$$s_i = \begin{cases} \dot{e}_i + \alpha e_i^{q/p}, & \text{if } s_i = 0 \text{ or } s_i \neq 0,\ |e_i| > \varepsilon, \\ \dot{e}_i^{p/q} + \alpha e_i, & \text{if } s_i \neq 0,\ |e_i| \leqslant \varepsilon, \end{cases} \tag{28}$$

where ε is a positive constant.

It can be seen from (24) and (25) that if $\mathbf{e}$ and $\dot{\mathbf{e}}$ are bounded, then $\mathbf{B}$ is bounded. Choose $\mathbf{K}$ such that $K_{ii} > |B_i|^*$, then

$$\dot{V} = \sum_{i=1}^{n} s_i[B_i - K_{ii}sgn(s_i)] < 0. \tag{29}$$

It is easy to verify that the terminal sliding condition can be satisfied under the condition $s_i \neq 0$.

3. MIMO AFTSMC for robotic manipulators

In this section, the MIMO AFTSMC for robotic manipulators is developed, which combines the advantages of the terminal sliding-mode control, the fuzzy inference mechanism, and the adaptive algorithm. First, the SISO FTSMC for robotic manipulators is derived, which establishes the FLC for proposed TSMC. Second, the MIMO FTSMC is proposed to deal with the model coupled of manipulators. Finally, a new MIMO AFTSMC method is presented. In this section, the adaptive law is designed and the stability of the overall system is proved based on the Lyapunov method.

3.1. SISO FTSMC for robotic manipulators

Although the aforementioned terminal sliding-mode controller can drive the system tracking error to converge to zero in finite time, it has several drawbacks. To guarantee that the system tracking error is convergent, each K_{ii} must be chosen so that it is very large. Unfortunately, this large control gain may cause undesired chattering. In this section, a single-input–single-output (SISO) FTSMC is developed to reduce the chattering.

From Eq. (17), choose the fuzzy logic controller gain $\mathbf{u}$ to replace the control input $\mathbf{K}sgn(\mathbf{s})$. The new control input can be expressed as

$$\boldsymbol{\tau} = -\mathbf{u}, \tag{30}$$

where $\mathbf{u} = [u_1, \ldots, u_i, \ldots, u_n]^T$. Therefore, the sign of u_i is chosen, which is the same as that of s_i. Substituting (30) into (18) leads to

$$\dot{V} = \mathbf{s}^T[\mathbf{B} - \mathbf{u}] = \sum_{i=1}^{n} s_i[B_i - u_i]. \tag{31}$$

Therefore, when $|s_i|$ is large, from (19) $|B_i|$ is also large so that $|u_i|$ must be given a large value. When $|s_i|$ is small, from (19) $|B_i|$ is also small so that $|u_i|$ can be of a smaller value. Then small $|u_i|$ will reduce the chattering. When s_i is zero, u_i can be zero; therefore, $\dot{V} = 0$. From these analyses, it is easy to make $\dot{V} \leqslant 0$ and guarantee the terminal sliding-mode of FTSMC. The fuzzy rules can be determined as follows:

IF s_i is NB, THEN u_i is NB
IF s_i is N, THEN u_i is N
IF s_i is Z, THEN u_i is Z
IF s_i is P, THEN u_i is P
IF s_i is PB, THEN u_i is PB

where s_i is the input variable of the fuzzy system and u_i is the output variable of the fuzzy system. Both are partitioned into five fuzzy subsets: negative big (NB), negative (N), zero (Z), positive (P), and positive big (PB). The triangular shape membership function of s_i is shown in Fig. 1a. The singleton membership function of u_i is shown in Fig. 1b. The main reasons of using triangular membership functions are adopted from literature [31–34]. First, under some assumptions about the probability density function of the input space, fuzzy partitions with triangular membership functions bring about entropy equalization. Second, the triangular membership functions with the 1/2 overlap between neighboring fuzzy sets lead to an error-free reconstruction. It is also worth noting that any deviation from the 1/2 overlap or modifications in the functional shape results in a nonzero reconstruction error. These characteristics are commonly used when interfacing fuzzy sets construct with numerical datum.

Choosing the weighted average defuzzification, the output of the fuzzy inference system can be written as

$$u_{ic} = \frac{\sum_{R=1}^{M} \theta_{iR}\mu_R(s_i)}{\sum_{R=1}^{M} \mu_R(s_i)}, \tag{32}$$

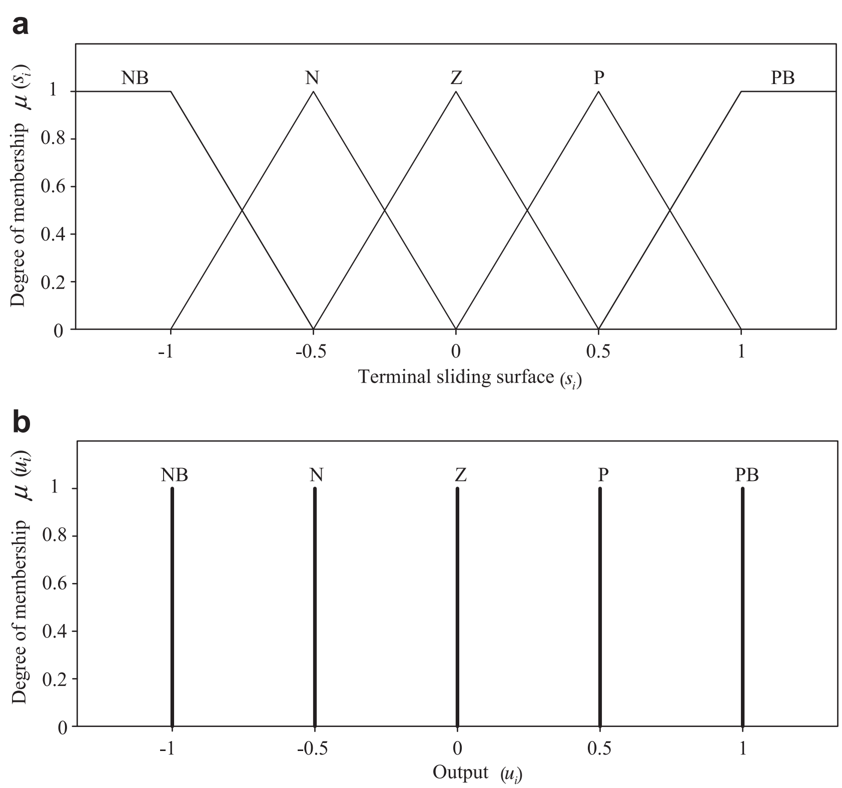

Fig. 1. (a) Input membership function; (b) output membership function.

where M is the number of rules, θ_{iR} is the associated singleton membership function of u_i and $\mu_R(s_i)$ is the strength of the Rth rule. Then, the output of the FTSMC for the robotic manipulators is

$$u_i = f_i \cdot u_{ic} \tag{33}$$

where f_i is the normalization factor of output variable.

The fuzzy terminal sliding condition can be satisfied as long as each f_i is chosen to be large enough such that

$$|f_i \cdot u_{ic}| > |B_i|^*, \tag{34}$$

then

$$\dot{V} = \sum_{i=1}^{n} s_i[B_i - u_i] = \sum_{i=1}^{n} s_i[B_i - f_i \cdot u_{ic}] < 0. \tag{35}$$

Thus, there is a guarantee that the system tracking error is quickly convergent under the condition $s_i \neq 0$.

3.2. MIMO FTSMC for robotic manipulators

In the SISO fuzzy system, each u_i is inferred by only an individual fuzzy system. To obtain a good performance, the coupling effect cannot be neglected, especially in robotic manipulators. In this section, the structure of MIMO fuzzy control scheme provides the ability not only to deal with the model coupled but also to enhance the system performance and robustness. The control diagram of the MIMO FTSMC is shown in Fig. 2.

The ith-output of the fuzzy inference system can be written as

$$u_{ic} = \frac{\sum_{R=1}^{M} \theta_{iR}\mu_R(s_i)}{\sum_{R=1}^{M} \mu_R(s_i)} = \mathbf{W}_i^T \boldsymbol{\theta}_i, \tag{36}$$

where M is the number of rules and $\boldsymbol{\theta}_i = [\theta_{i1}, \ldots, \theta_{ii}, \ldots, \theta_{iM}]$ is the consequent parameter; and $\mathbf{W}_i^T = [w_{i1}, \ldots, w_{iR}, \ldots, w_{iM}]^T$ with each variable w_{iR} as the fuzzy basis function is defined as

$$w_{iR} = \frac{\mu_R(s_i)}{\sum_{R=1}^{M} \mu_R(s_i)}. \tag{37}$$

Then, the ith-output of the MIMO FTSMC for robotic manipulators can be expressed as

$$u_i = \sum_{j=1}^{n} f_{ij} \cdot u_{jc}, \tag{38}$$

where f_{ij} is the normalization factor of the jth-output of the fuzzy inference system for ith-output variable. The fuzzy terminal sliding condition can be satisfied as long as each f_{ij} is chosen to be large enough such that

$$\left|\sum_{j=1}^{n} f_{ij} \cdot u_{jc}\right| > |B_i|^*, \tag{39}$$

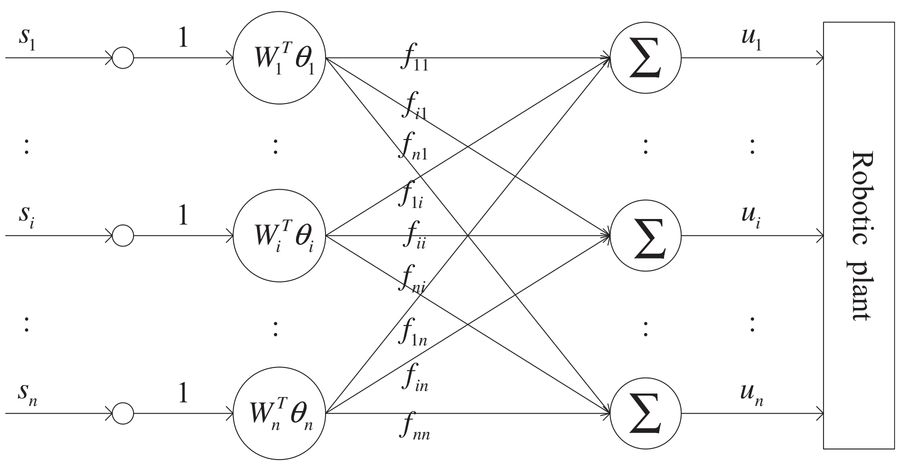

Fig. 2. The structure of a MIMO FTSMC.

then

$$\dot{V} = \sum_{i=1}^{n} s_i[B_i - u_i] = \sum_{i=1}^{n} s_i\left[B_i - \sum_{j=1}^{n} f_{ij} \cdot u_{jc}\right] < 0. \tag{40}$$

Thus, there is a guarantee that the system tracking error is quickly convergent under the condition $s_i \neq 0$.

3.3. MIMO AFTSMC for robotic manipulators

Although MIMO FTSMC is an effective method, its major disadvantage is that the output normalization factor of the output of the fuzzy controller should have been previously tuned by trial-and-error procedures. To overcome this problem, this subsection presents a new MIMO AFTSMC for robotic manipulators. The adaptive law is designed on the basis of the Lyapunov stability criterion. The normalization factor of output variable in the fuzzy mechanism and the output value of the compensator are adapted online to improve the performance of the FTSMC. The basic architecture of the MIMO AFTSMC is shown in Fig. 3.

Let the output of the MIMO AFTSMC for robotic manipulators be

$$\boldsymbol{\tau} = -\mathbf{u} - \boldsymbol{\rho}\mathbf{s}. \tag{41}$$

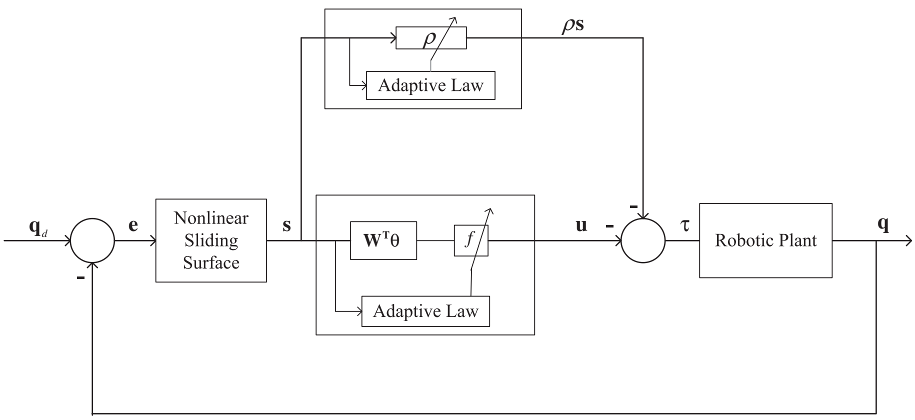

Fig. 3. The architecture of MIMO AFTSMC for robotic manipulators.

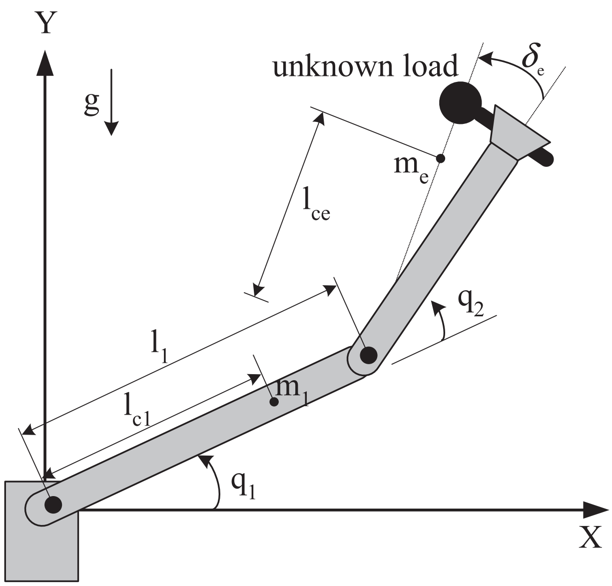

Fig. 4. An articulated two-link manipulator.

The adaptive fuzzy controller output is $\mathbf{u} = \mathbf{f} \cdot \mathbf{u}_c$ in which $\mathbf{u}_c$ is output of the fuzzy inference system and $\mathbf{f}$ is the normalization factor of output variable. The output value of the compensator is $\boldsymbol{\rho}\mathbf{s}$, where $\boldsymbol{\rho} = diag[a_1 + \sigma_1, \ldots, a_i + \sigma_i, \ldots, a_n + \sigma_n]$ is a diagonal positive definite matrix in which a_i is a positive constant, and σ_i is a positive value.

Substituting (41) into (1) yields

$$\mathbf{H}\dot{\mathbf{s}} = -\mathbf{C}\mathbf{s} + \mathbf{B} - \mathbf{u} - \boldsymbol{\rho}\mathbf{s}. \tag{42}$$

Define $\mathbf{f}^*$ as the optimal estimation normalization factor for $\mathbf{B}$. Then, there exists the optimal estimation error $w_i > 0$ $(i = 1, \ldots, n)$ satisfying

$$\left| B_i - \sum_{j=1}^{n} f_{ij}^* \cdot u_{jc} \right| \leqslant w_i \quad (i = 1, \ldots, n). \tag{43}$$

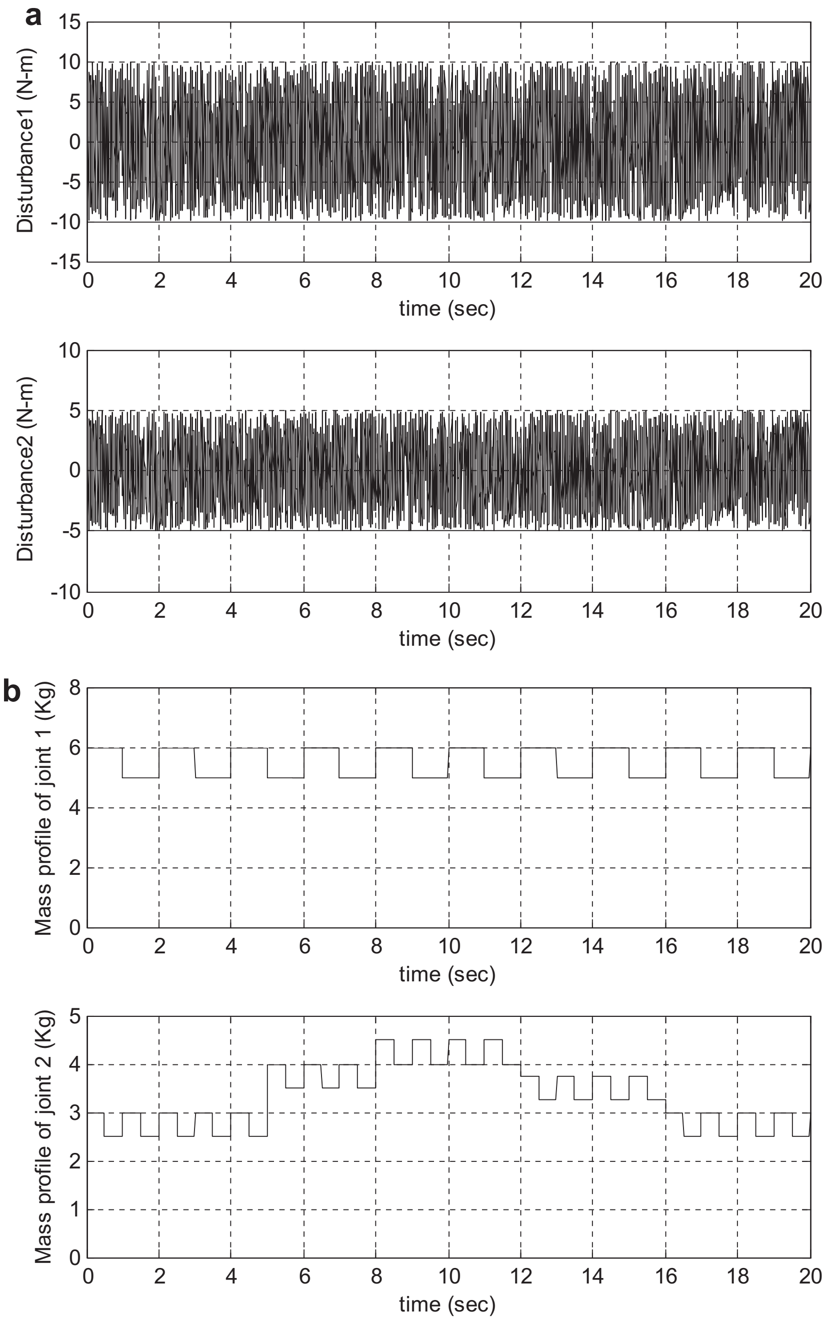

Fig. 5. (a) The disturbance profiles; (b) the uncertain mass of the joints.

Define the error of the normalization factor of the fuzzy output variable as

$$\tilde{f}_{ij} = f_{ij} - f_{ij}^*. \tag{44}$$

Then

$$\sum_{j=1}^{n} f_{ij} \cdot u_{jc} = \sum_{j=1}^{n} \tilde{f}_{ij} \cdot u_{jc} + \sum_{j=1}^{n} f_{ij}^* \cdot u_{jc}. \tag{45}$$

Define $\sigma_i^*|s_i|$ as the upper boundary of the compensation for optimal estimation error w_i. That is

$$w_i \leqslant \sigma_i^*|s_i| \quad (i = 1, \ldots, n). \tag{46}$$

And let $\sigma_i|s_i|$ be the compensation value for optimal estimation error w_i.

Table 1
The control parameters.

Controller	Control law	Adaptive law	Sliding surface	q	p	$\boldsymbol{\alpha}, \boldsymbol{\lambda}$	γ_{ij}, σ_i	ε
MIMO AFTSMC	$\boldsymbol{\tau} = -\mathbf{u} - \boldsymbol{\rho}\mathbf{s}$ $u_i = \sum_{j=1}^n f_{ij} \cdot u_{jc}$ $\rho_i = a_i + \sigma_i$	$\dot{f}_{ij} = \dot{\tilde{f}}_{ij} = \gamma_{ij} s_i u_{jc}$ $\dot{\sigma}_i = \dot{\tilde{\sigma}}_i = \eta_i s_i^2$	$\mathbf{s} = \dot{\mathbf{e}} + \boldsymbol{\alpha} e^{q/p}$	5	7	$\begin{bmatrix} 20 & 0 \\ 0 & 20 \end{bmatrix}$	$\gamma_{11} = \gamma_{22} = 100$ $\gamma_{12} = 80$ $\gamma_{21} = 800$ $\sigma_1 = \sigma_2 = 1$	0.01
MIMO AFSMC	$\boldsymbol{\tau} = -\mathbf{u} - \boldsymbol{\rho}\mathbf{s}$ $u_i = \sum_{j=1}^n f_{ij} \cdot u_{jc}$ $\rho_i = a_i + \sigma_i$	$\dot{f}_{ij} = \dot{\tilde{f}}_{ij} = \gamma_{ij} s_i u_{jc}$ $\dot{\sigma}_i = \dot{\tilde{\sigma}}_i = \eta_i s_i^2$	$\mathbf{s} = \dot{\mathbf{e}} + \lambda e$	–	–	$\begin{bmatrix} 20 & 0 \\ 0 & 20 \end{bmatrix}$	$\gamma_{11} = \gamma_{22} = 100$ $\gamma_{12} = 80$ $\gamma_{21} = 800$ $\sigma_1 = \sigma_2 = 1$	–
SISO AFTSMC	$\boldsymbol{\tau} = -\mathbf{u} - \boldsymbol{\rho}\mathbf{s}$ $u_i = f_i \cdot u_{ic}$ $\rho_i = a_i + \sigma_i$	$\dot{f}_i = \dot{\tilde{f}}_i = \gamma_i s_i u_{ic}$ $\dot{\sigma}_i = \dot{\tilde{\sigma}}_i = \eta_i s_i^2$	$\mathbf{s} = \dot{\mathbf{e}} + \boldsymbol{\alpha} e^{q/p}$	5	7	$\begin{bmatrix} 20 & 0 \\ 0 & 20 \end{bmatrix}$	$\gamma_1 = \gamma_2 = 100$ $\sigma_1 = \sigma_2 = 1$	0.01
SISO AFSMC	$\boldsymbol{\tau} = -\mathbf{u} - \boldsymbol{\rho}\mathbf{s}$ $u_i = f_i \cdot u_{ic}$ $\rho_i = a_i + \sigma_i$	$\dot{f}_i = \dot{\tilde{f}}_i = \gamma_i s_i u_{ic}$ $\dot{\sigma}_i = \dot{\tilde{\sigma}}_i = \eta_i s_i^2$	$\mathbf{s} = \dot{\mathbf{e}} + \lambda e$	–	–	$\begin{bmatrix} 20 & 0 \\ 0 & 20 \end{bmatrix}$	$\gamma_1 = \gamma_2 = 100$ $\sigma_1 = \sigma_2 = 1$	–

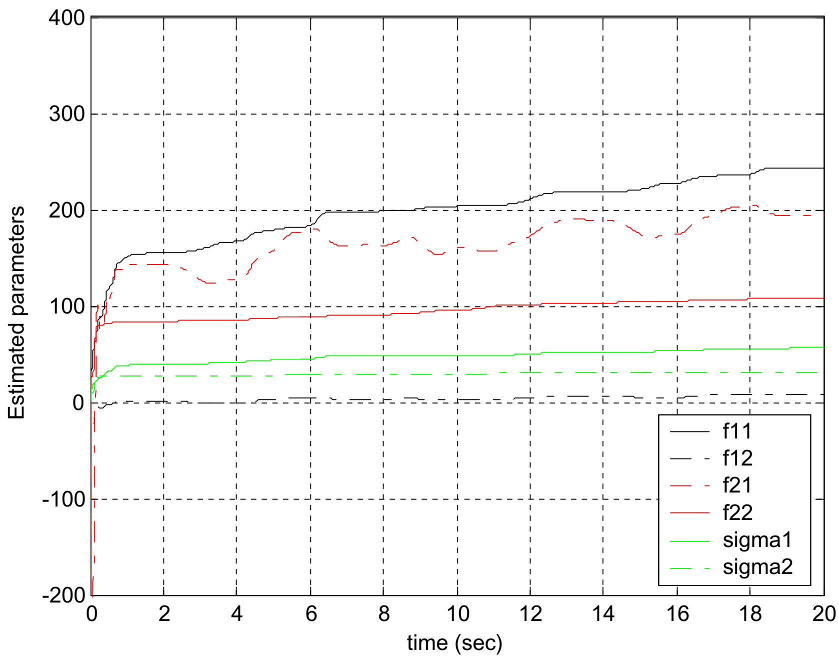

Fig. 6. Curves of estimated parameters.

Define

$$\tilde{\sigma}_i = \sigma_i - \sigma_i^* \quad (i = 1, \ldots, n). \tag{47}$$

Choose the Lyapunov function candidate as

$$V = \frac{1}{2}(\mathbf{s}^T\mathbf{H}\mathbf{s}) + \frac{1}{2}\sum_{i=1}^{n}\sum_{j=1}^{n}\frac{1}{2\gamma_{ij}}\tilde{f}_{ij}^2 + \sum_{i=1}^{n}\frac{1}{2\eta_i}\tilde{\sigma}_i^2, \tag{48}$$

where $\mathbf{H}$ is a symmetric positive definite matrix, $\tilde{f}_{ij}^2 > 0$ and $\tilde{\sigma}_i^2 > 0$, γ_{ij} and η_i are positive constants; therefore, V is positive definite. Consider the derivative of V

$$\begin{aligned}\dot{V} &= \frac{1}{2}\left(\dot{\mathbf{s}}^T\mathbf{H}\mathbf{s} + \mathbf{s}^T\dot{\mathbf{H}}\mathbf{s} + \mathbf{s}^T\mathbf{H}\dot{\mathbf{s}}\right) + \sum_{i=1}^{n}\sum_{j=1}^{n}\frac{1}{\gamma_{ij}}\tilde{f}_{ij}\dot{\tilde{f}}_{ij} + \sum_{i=1}^{n}\frac{1}{\eta_i}\tilde{\sigma}_i\dot{\tilde{\sigma}}_i = \mathbf{s}^T[\mathbf{H}\dot{\mathbf{s}} + \mathbf{C}\mathbf{s}] + \sum_{i=1}^{n}\sum_{j=1}^{n}\frac{1}{\gamma_{ij}}\tilde{f}_{ij}\dot{\tilde{f}}_{ij} + \sum_{i=1}^{n}\frac{1}{\eta_i}\tilde{\sigma}_i\dot{\tilde{\sigma}}_i \\ &= \mathbf{s}^T[-\mathbf{C}\mathbf{s} + \mathbf{B} - \mathbf{u} - \boldsymbol{\rho}\mathbf{s} + \mathbf{C}\mathbf{s}] + \sum_{i=1}^{n}\sum_{j=1}^{n}\frac{1}{\gamma_{ij}}\tilde{f}_{ij}\dot{\tilde{f}}_{ij} + \sum_{i=1}^{n}\frac{1}{\eta_i}\tilde{\sigma}_i\dot{\tilde{\sigma}}_i = \mathbf{s}^T[\mathbf{B} - \mathbf{u} - \boldsymbol{\rho}\mathbf{s}] + \sum_{i=1}^{n}\sum_{j=1}^{n}\frac{1}{\gamma_{ij}}\tilde{f}_{ij}\dot{\tilde{f}}_{ij} + \sum_{i=1}^{n}\frac{1}{\eta_i}\tilde{\sigma}_i\dot{\tilde{\sigma}}_i \\ &= \sum_{i=1}^{n} s_i\left[B_i - \sum_{j=1}^{n} f_{ij}u_{jc} - a_i s_i - \sigma_i s_i\right] + \sum_{i=1}^{n}\sum_{j=1}^{n}\frac{1}{\gamma_{ij}}\tilde{f}_{ij}\dot{\tilde{f}}_{ij} + \sum_{i=1}^{n}\frac{1}{\eta_i}\tilde{\sigma}_i\dot{\tilde{\sigma}}_i.\end{aligned} \tag{49}$$

As $\sum_{j=1}^{n} f_{ij}u_{jc} = \sum_{j=1}^{n}\tilde{f}_{ij}u_{jc} + \sum_{j=1}^{n} f_{ij}^* u_{jc}$, then Eq. (49) becomes

$$\begin{aligned}\dot{V} &= \sum_{i=1}^{n} s_i\left[B_i - \left(\sum_{j=1}^{n}\tilde{f}_{ij}u_{jc} + \sum_{j=1}^{n} f_{ij}^* u_{jc}\right) - a_i s_i - (\tilde{\sigma}_i s_i + \sigma_i^* s_i)\right] + \sum_{i=1}^{n}\sum_{j=1}^{n}\frac{1}{\gamma_{ij}}\tilde{f}_{ij}\dot{\tilde{f}}_{ij} + \sum_{i=1}^{n}\frac{1}{\eta_i}\tilde{\sigma}_i\dot{\tilde{\sigma}}_i \\ &= \sum_{i=1}^{n} -s_i\ a_i s_i + \sum_{i=1}^{n}\left[s_i\left(B_i - \sum_{j=1}^{n} f_{ij}^* u_{jc}\right) - s_i\sigma_i^* s_i\right] + \sum_{i=1}^{n}\left(\sum_{j=1}^{n}\frac{1}{\gamma_{ij}}\tilde{f}_{ij}\dot{\tilde{f}}_{ij} - s_i\sum_{j=1}^{n}\tilde{f}_{ij}u_{jc}\right) + \sum_{i=1}^{n}\left(\frac{1}{\eta_i}\tilde{\sigma}_i\dot{\tilde{\sigma}}_i - s_i\tilde{\sigma}_i s_i\right).\end{aligned} \tag{50}$$

As $s_i\left(B_i - \sum_{j=1}^{n} f_{ij}^* u_{jc}\right) \leqslant |s_i|\left|B_i - \sum_{j=1}^{n} f_{ij}^* \cdot u_{jc}\right| \leqslant |s_i| w_i$, the equation becomes

$$\dot{V} \leqslant \sum_{i=1}^{n} -s_i a_i s_i + \sum_{i=1}^{n}\left(|s_i| w_i - s_i\sigma_i^* s_i\right) + \sum_{i=1}^{n}\sum_{j=1}^{n}\tilde{f}_{ij}\left(\frac{1}{\gamma_{ij}}\dot{\tilde{f}}_{ij} - s_i u_{jc}\right) + \sum_{i=1}^{n}\tilde{\sigma}_i\left(\frac{1}{\eta_i}\dot{\tilde{\sigma}}_i - s_i^2\right). \tag{51}$$

As $w_i \leqslant \sigma_i^*|s_i|$

$$|s_i| w_i \leqslant \sigma_i^*|s_i||s_i| = \sigma_i^*|s_i|^2 = \sigma_i^* s_i^2. \tag{52}$$

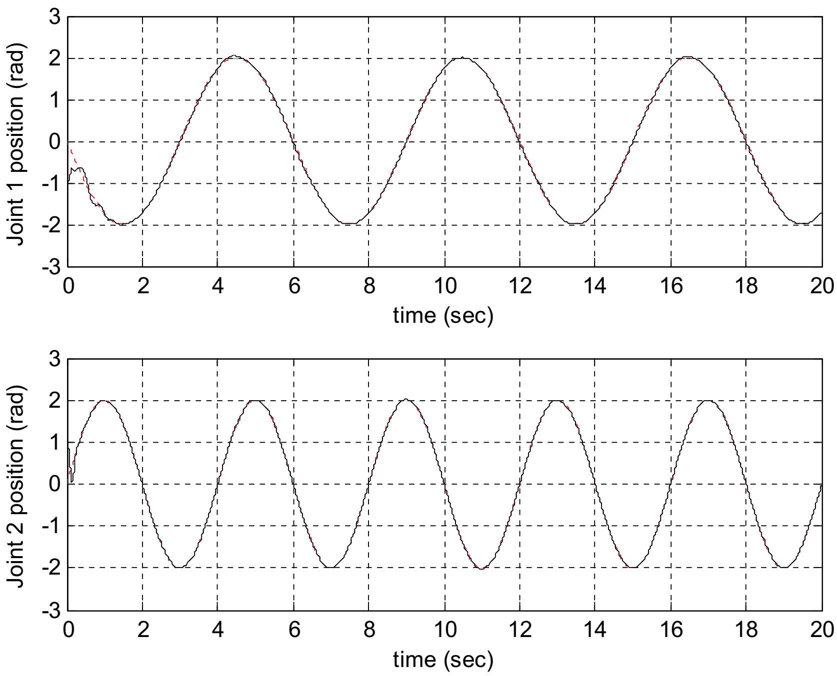

Fig. 7. Responses of the joint angles under MIMO AFTSMC. (Dotted line: desired trajectory, solid line: actual trajectory).

Therefore

$$\dot{V} \leqslant \sum_{i=1}^{n} -s_i a_i s_i + \sum_{i=1}^{n}\sum_{j=1}^{n}\tilde{f}_{ij}\left(\frac{1}{\gamma_{ij}}\dot{\tilde{f}}_{ij} - s_i u_{jc}\right) + \sum_{i=1}^{n}\tilde{\sigma}_i\left(\frac{1}{\eta_i}\dot{\tilde{\sigma}}_i - s_i^2\right). \tag{53}$$

If the adaptive laws are chosen as

$$\dot{f}_{ij} = \dot{\tilde{f}}_{ij} = \gamma_{ij} s_i u_{jc}, \tag{53a}$$

$$\dot{\sigma}_i = \dot{\tilde{\sigma}}_i = \eta_i s_i^2, \tag{53b}$$

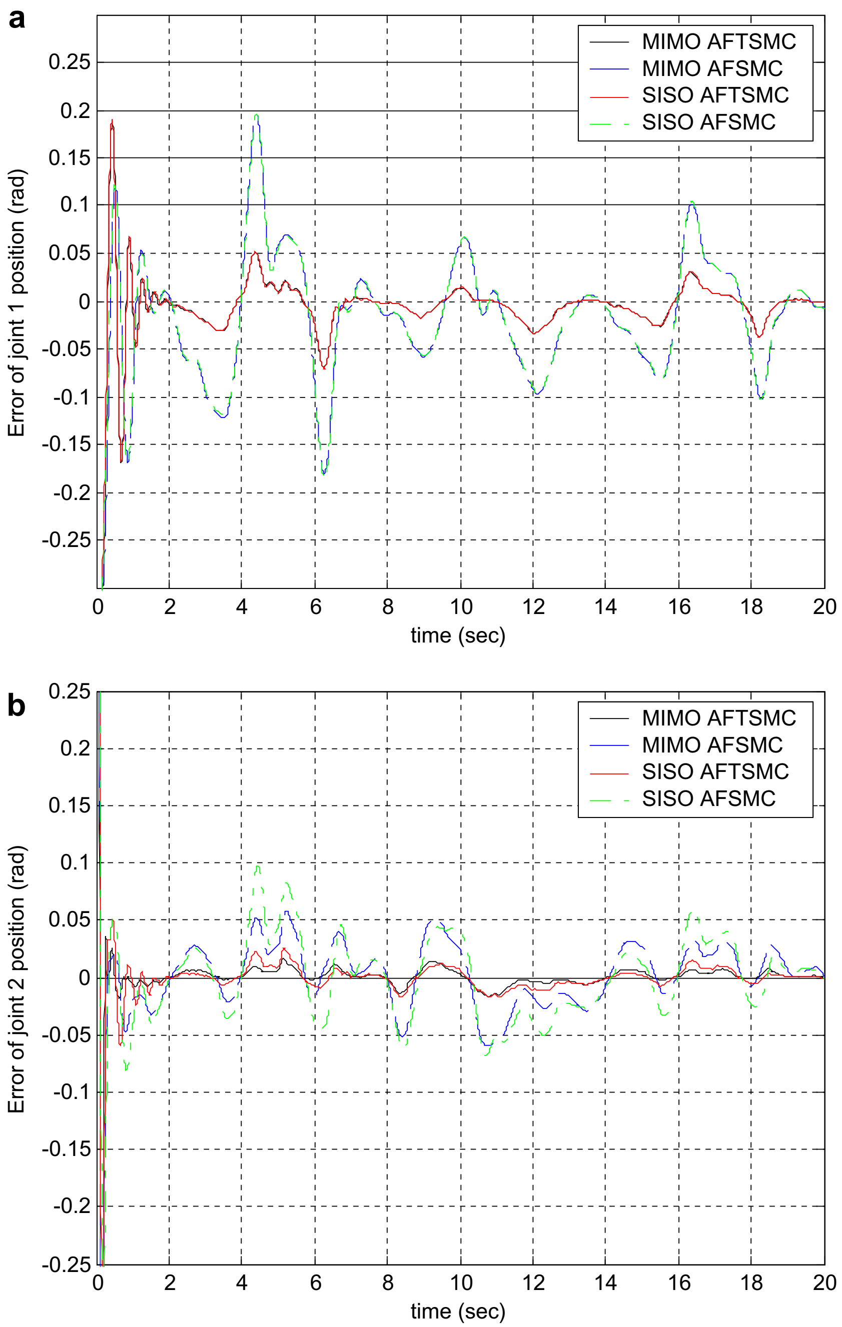

Fig. 8. (a) Tracking errors of joint 1; (b) tracking errors of joint 2. (Solid line: MIMO AFTSMC, dashed line: MIMO AFSMC, dotted line: SISO AFTSMC, dash-dot line: SISO AFSMC).

then

$$\dot{V} \leqslant \sum_{i=1}^{n} -s_i a_i s_i \leqslant 0. \tag{54}$$

Because a_i ($i = 1,\ldots,n$) is a positive constant, $\dot{V} < 0$ when $\mathbf{s} \neq 0$. Thus, the controller with the adaptive law in (53) can drive the system tracking error to converge to zero in finite time, which is $\dot{\mathbf{e}} + \alpha \mathbf{e}^{q/p} \to 0$ as $t \to t'$ where t' can be any finite time. In other words, $\mathbf{q} \to \mathbf{q}_d,\ \dot{\mathbf{q}} \to \dot{\mathbf{q}}_d$, as $t \to t'$. Therefore, it is proved that, with the MIMO adaptive fuzzy terminal sliding-mode control input (41), the actual joint positions reach the desired trajectory in finite time.

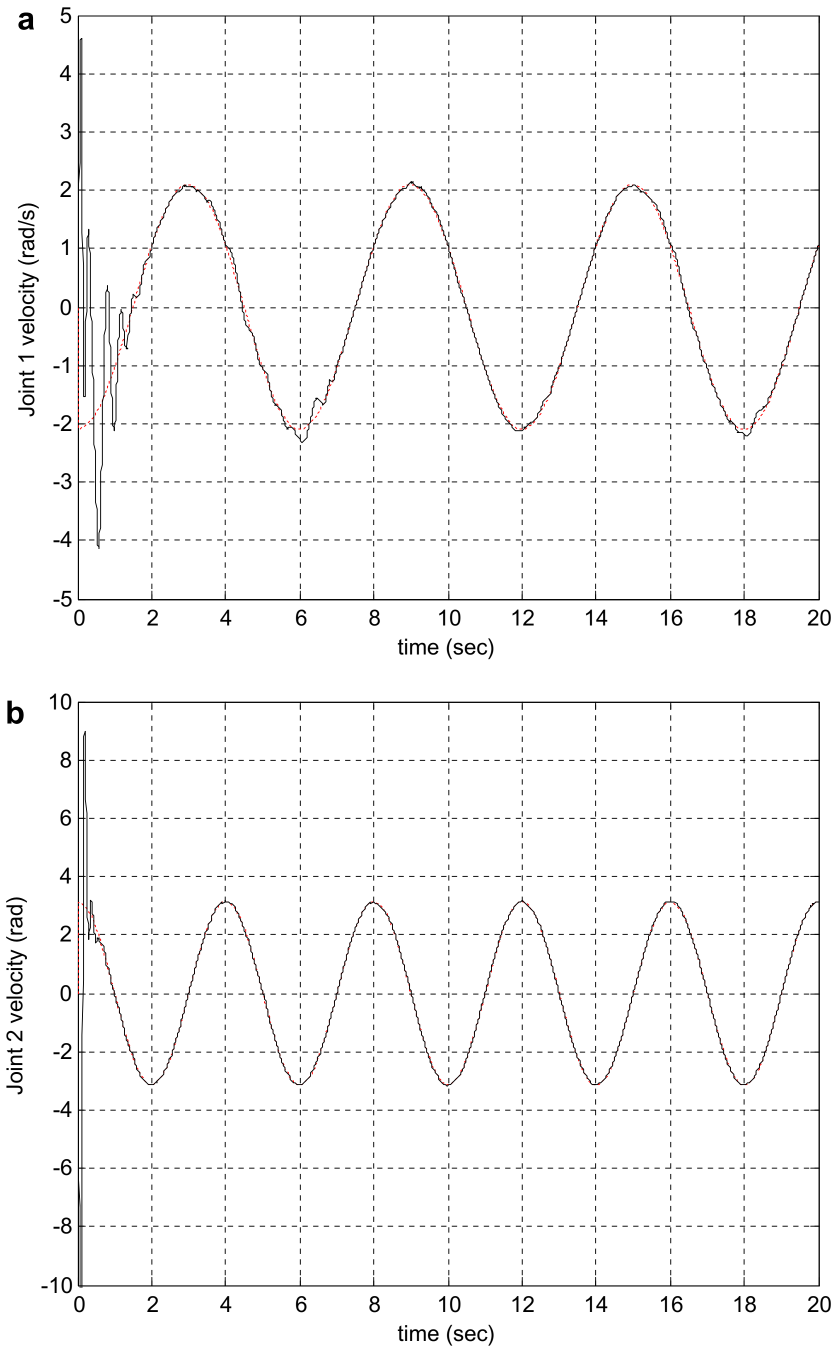

Fig. 9. (a) Joint 1 velocity under MIMO AFTSMC; (b) joint 2 velocity under MIMO AFTSMC. (Dotted line: desired velocity trajectory, solid line: actual velocity trajectory).

Remark 2 ([5,7,38]). For evaluating the performance of the controller, we can use the performance criteria as follows:

(a) Integral of the absolute value of the error (IAE)

$$\mathrm{IAE} = \int_0^{t_f} |e(t)|dt. \tag{55}$$

(b) Integral of the time multiplied by the absolute value of the error (ITAE)

$$\mathrm{ITAE} = \int_0^{t_f} t \cdot |e(t)|dt. \tag{56}$$

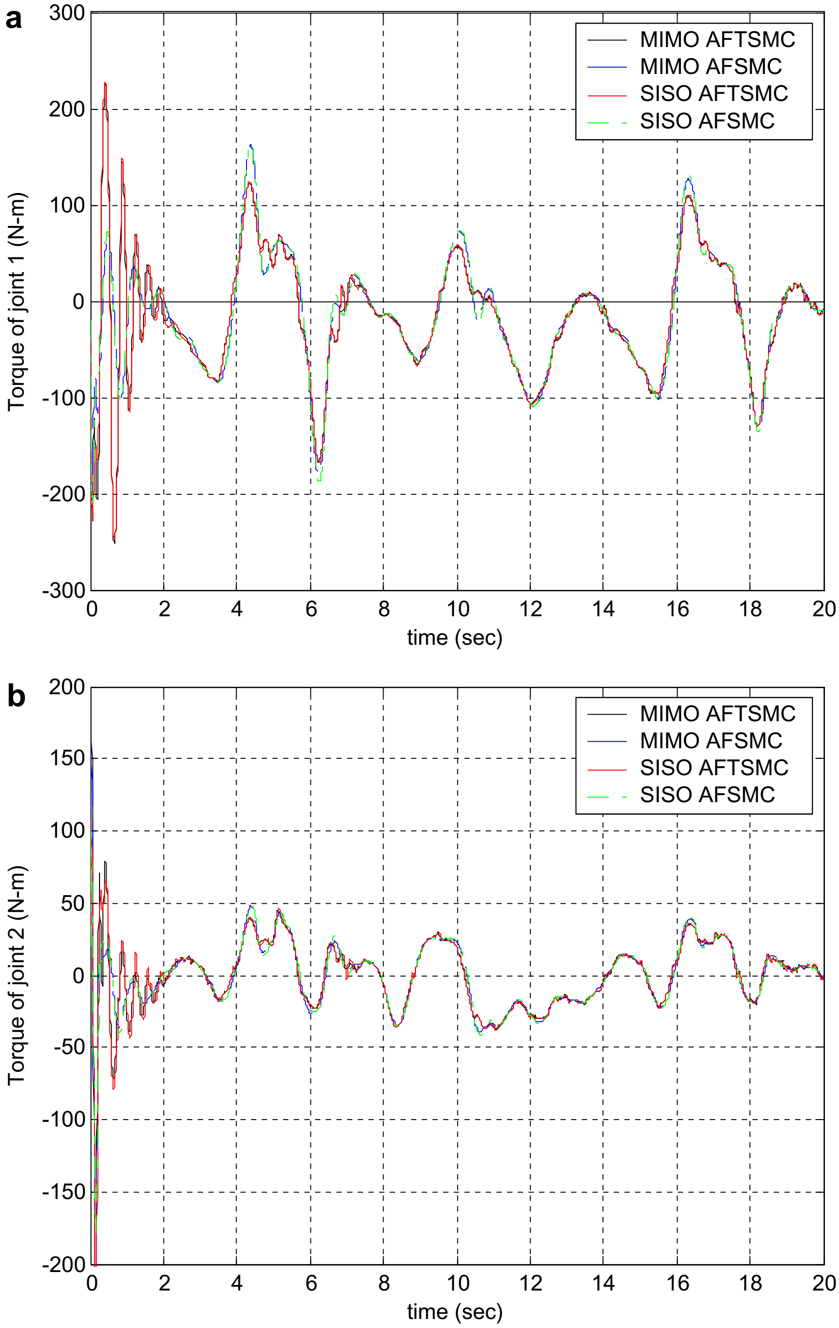

Fig. 10. (a) The control input 1; (b) the control input 2. (Solid line: MIMO AFTSMC, dashed line: MIMO AFSMC, dotted line: SISO AFTSMC, dash-dot line: SISO AFSMC).

(c) Integral of the square value (ISV) of the control input

$$\mathrm{ISV} = \int_0^{t_f} u^2(t)dt. \tag{57}$$

Both IAE and ITAE are used as objective numerical measures of tracking performance for an entire error curve, where t_f represents the total running time. The criterion IAE will give an intermediate result. In ITAE, time appears as a factor; it will heavily emphasize errors that occur late in time. The criterion ISV shows the consumption of energy.

4. Simulation examples

Consider the two-link manipulators, as shown in Fig. 4. The dynamical equation of the manipulators can be described as [39,40]

$$\begin{bmatrix} H_{11} & H_{12} \\ H_{21} & H_{22} \end{bmatrix}\begin{bmatrix} \ddot{q}_1 \\ \ddot{q}_2 \end{bmatrix} + \begin{bmatrix} -h\dot{q}_2 & -h(\dot{q}_1+\dot{q}_2) \\ h\dot{q}_1 & 0 \end{bmatrix}\begin{bmatrix} \dot{q}_1 \\ \dot{q}_2 \end{bmatrix} + \begin{bmatrix} G_1 \\ G_2 \end{bmatrix} + \begin{bmatrix} T_{d1} \\ T_{d2} \end{bmatrix} = \begin{bmatrix} \tau_1 \\ \tau_2 \end{bmatrix},$$

where

$$H_{11} = c_1 + 2c_3\cos q_2 + 2c_4\sin q_2, \quad H_{12} = H_{21} = c_2 + c_3\cos q_2 + c_4\sin q_2, \quad H_{22} = c_2,$$
$$h = c_3\sin q_2 - c_4\cos q_2, \quad G_1 = b_1\cos q_1 + b_2\cos(q_1+q_2), \quad G_2 = b_2\cos(q_1+q_2)$$

Table 2
The performance indices.

Controller	Joint	Example 1			Example 2		
		IAE (rad)	ITAE (rad-s)	ISV (N-m)^2	IAE (rad)	ITAE (rad-s)	ISV (N-m)^2
MIMO	Joint 1	0.4325	2.2045	85,392	0.5256	3.6151	113,030
AFTSMC	Joint 2	0.1889	0.8472	16,772	0.1235	0.4425	11,909
MIMO	Joint 1	1.0809	8.1813	74,148	1.3626	11.4203	103,790
AFSMC	Joint 2	0.5385	4.1116	13,008	0.3188	1.9016	9064
SISO	Joint 1	0.4329	2.2062	85,806	0.5305	3.6913	109,680
AFTSMC	Joint 2	0.2369	1.1414	13,854	0.2613	1.6754	10,072
SISO	Joint 1	1.0711	8.1282	76,099	1.3926	11.5821	101,350
AFSMC	Joint 2	0.6719	5.2541	11,013	0.8069	6.4714	8177

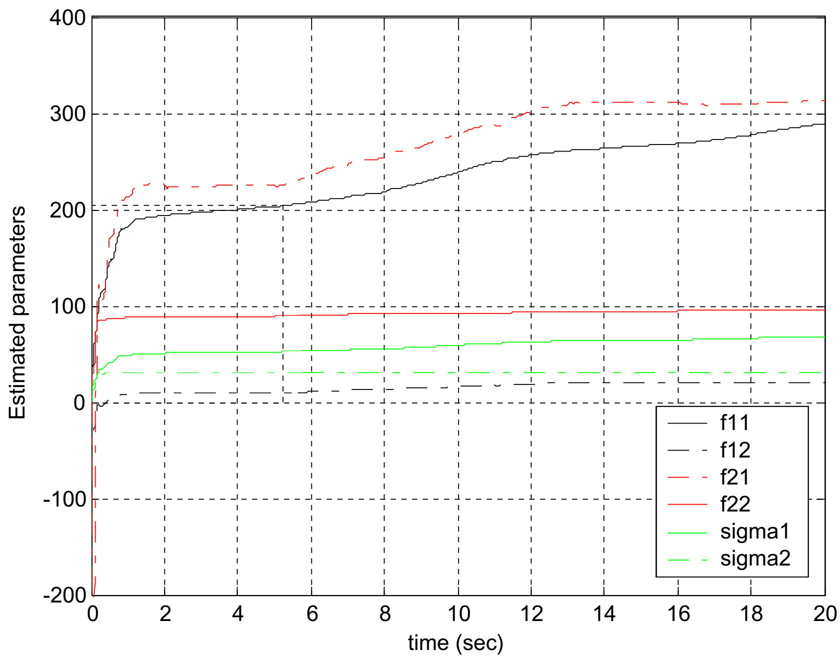

Fig. 11. Curves of estimated parameters.

with

$$c_1 = I_1 + m_1 l_{c1}^2 + I_e + m_e l_{ce}^2 + m_e l_1^2, \quad c_2 = I_e + m_e l_{ce}^2, \quad c_3 = m_e l_1 l_{ce} \cos \delta_e, \quad c_4 = m_e l_1 l_{ce} \sin \delta_e,$$
$$b_1 = m_1 g l_{c1} + m_e g l_1, \quad b_2 = m_e g l_{ce}.$$

The nominal parameters of the two-link manipulators are chosen as follows:

$$m_1 = 5kg, \quad m_e = 2.5kg, \quad l_1 = 1.0m, \quad l_{c1} = 0.5m, \quad l_{ce} = 0.5m, \quad \delta_e = 0^\circ, \quad I_1 = 0.36Kgm^2, \quad I_2 = 0.24Kgm^2.$$

The disturbance $\mathbf{T}_d$ is a random signal; Fig. 5a depicts the disturbance profiles. The uncertain mass of joints 1 and 2 is illustrated in Fig. 5b; it can be seen that the load of the manipulators is changed at $t = 5, 8, 12, 16$ s, respectively.

Two examples, both periodic and nonperiodic trajectories, are given in this section to illustrate the effectiveness of the proposed approach. All the control laws and the parameters of these four controllers are listed in Table 1. The initial estimated parameters are chosen as $f_{11} = f_{12} = f_{21} = f_{22} = 0$, $a_1 = a_2 = 1$, $\sigma_1 = \sigma_2 = 0$. The sampling time used in the simulation is 5 ms.

4.1. Example 1

The desired joint trajectories for tracking are

$$\begin{bmatrix} q_{d1} \\ q_{d2} \end{bmatrix} = \begin{bmatrix} -2\sin\left(\frac{1}{3}\pi t\right) \\ 2\sin\left(\frac{1}{2}\pi t\right) \end{bmatrix} rad.$$

In this example, we apply the proposed MIMO AFTSMC, the SISO AFTSMC, the classical MIMO AFSMC, and the classical SISO AFSMC to the robotic manipulator, respectively. The system initial states are chosen as $q_1(0) = -1$, $q_2(0) = 1$, $\dot{q}_1(0) = \dot{q}_2(0) = 0$.

The curves of the estimated parameters are shown in Fig. 6. The responses of the joint angles under the proposed MIMO AFTSMC are illustrated in Fig. 7, and one can find that the proposed controller provides a reasonable tracking capability in the various uncertainties. The tracking errors of joints 1 and 2 under these four controllers are depicted in Fig. 8; the tracking error convergence speed for the proposed MIMO AFTSMC is faster than that of the three other controllers. The joint velocities under the proposed MIMO AFTSMC are shown in Fig. 9, while the corresponding control inputs are shown in Fig. 10. The performance indices are tabulated in Table 2.

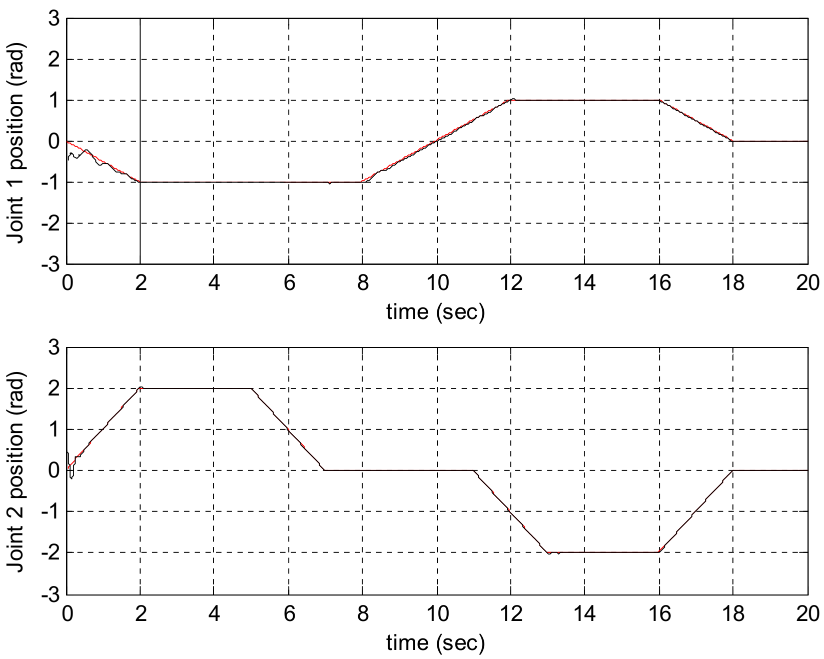

Fig. 12. Responses of the joint angles under MIMO AFTSMC. (Dotted line: desired trajectory, solid line: actual trajectory).

4.2. Example 2

The nonperiodic trajectories for tracking are shown in Fig. 12. In this example, the system initial states are chosen as $q_1(0) = -0.5,\ q_2(0) = 0.5,\ \dot{q}_1(0) = \dot{q}_2(0) = 0$.

The curves of the estimated parameters are shown in Fig. 11. The responses of the joint angles under the proposed MIMO AFTSMC are illustrated in Fig. 12, and one can find that the proposed controller provides a fast tracking capability in the various uncertainties. The tracking errors of joints 1 and 2 under these four controllers are depicted in Fig. 13. The joint velocities under the proposed MIMO AFTSMC are shown in Fig. 14, while the corresponding control inputs are shown in Fig. 15. The performance indices are tabulated in Table 2.

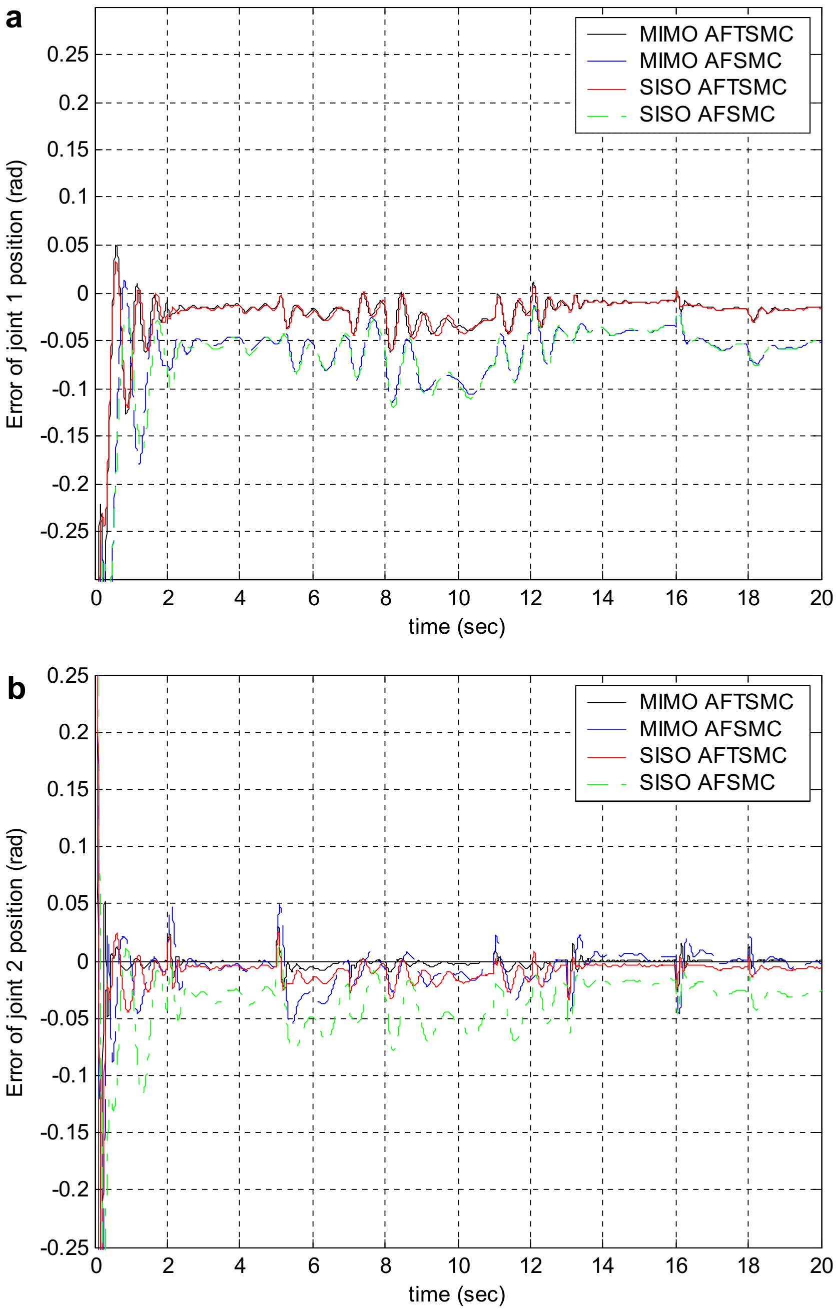

Fig. 13. (a) Tracking errors of joint 1; (b) tracking errors of joint 2. (Solid line: MIMO AFTSMC, dashed line: MIMO AFSMC, dotted line: SISO AFTSMC, dash-dot line: SISO AFSMC).

From Figs. 6, 7, 11 and 12, without any expert knowledge, one can see that the MIMO AFTSMC possesses an excellent tracking performance after a short learning period. By comparing to Figs. 8 and 13 and Table 2, one can conclude that the tracking performance of the proposed MIMO AFTSMC is superior to that of the three other controllers. From Figs. 9 and 14, one can find that the proposed controller shows the joint movement with high acceleration. It is obvious from Figs. 10 and 15 and Table 2 that the magnitude of control torques are almost the same.

5. Conclusions

In this study, a MIMO AFTSMC for robotic manipulators has been developed, which integrates the MIMO FLC, the TSMC, and the adaptive scheme. The combined scheme is shown to have the merits of these approaches. This control algorithm is

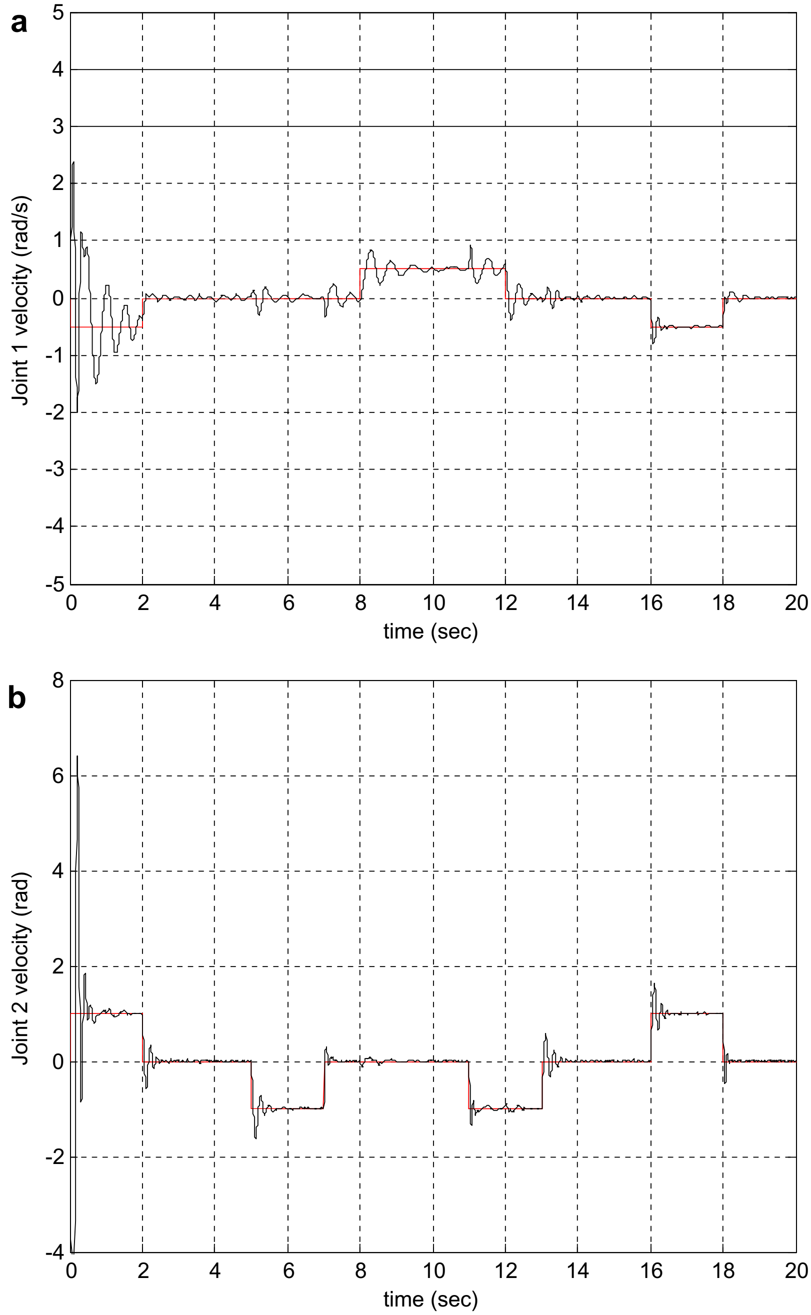

Fig. 14. (a) Joint 1 velocity under MIMO AFTSMC; (b) joint 2 velocity under MIMO AFTSMC. (Dotted line: desired velocity trajectory, solid line: actual velocity trajectory).

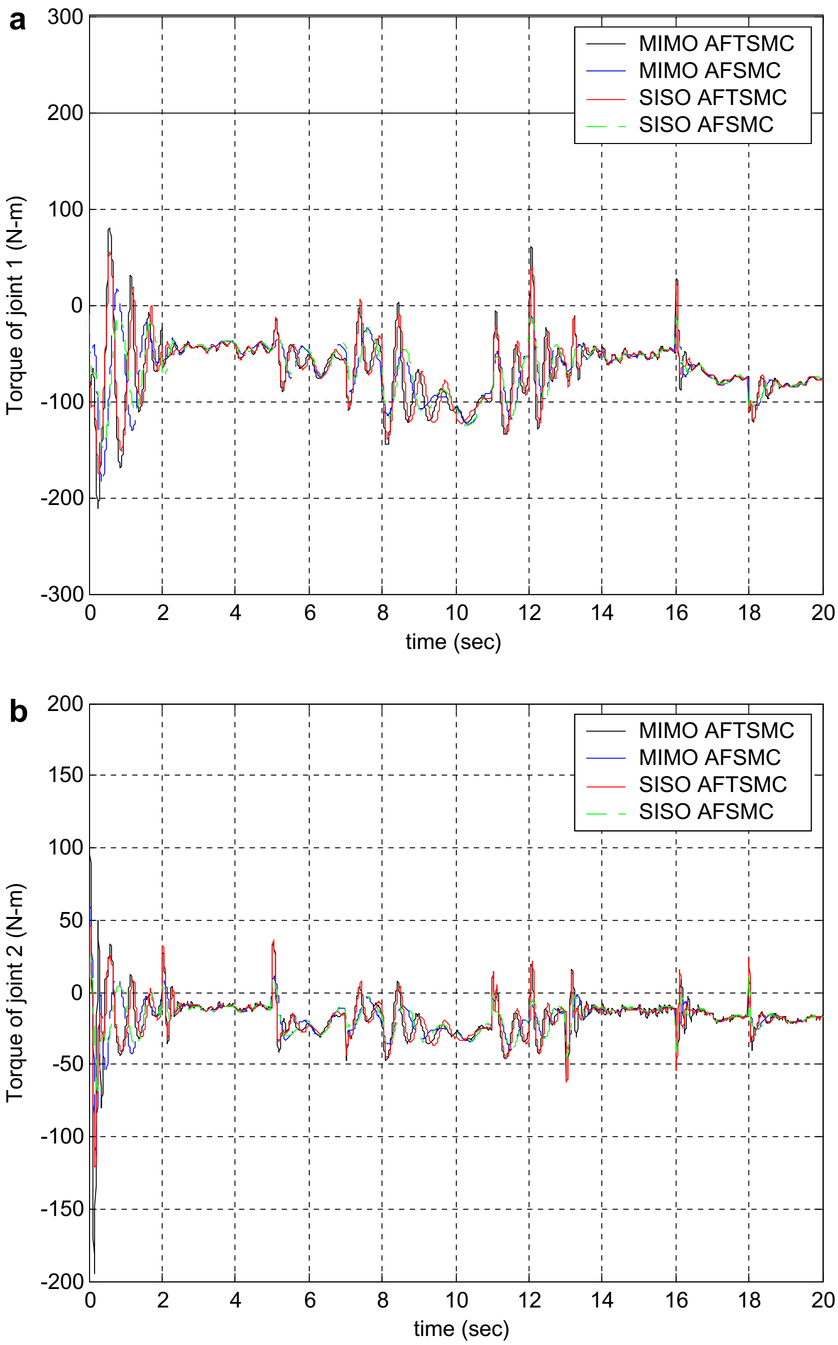

Fig. 15. (a) The control input 1; (b) the control input 2. (Solid line: MIMO AFTSMC, dashed line: MIMO AFSMC, dotted line: SISO AFTSMC, dash-dot line: SISO AFSMC).

designed on the basis of the Lyapunov stability criterion, which can be applied to *n*-link robotic manipulators with unmodeled dynamics and uncertainties. The proposed MIMO AFTSMC is shown to have the following four characteristics. First, the scheme presented can drive the system tracking error to converge to zero in finite time. Second, the proposed scheme can eliminate the chattering of the TSMC schemes and reduce the rule number of the FLC. Third, the adaptive scheme does not require prior knowledge of dynamic parameters. Finally, the control algorithm can be applied to *n*-link robotic manipulators with unmodeled dynamics, unstructured uncertainties, and external disturbances. The effectiveness and the validity of the MIMO AFTSMC have been demonstrated by computer simulations. The proposed control can achieve the best performance in comparison with the SISO AFSMC, the SISO AFTSMC, and the MIMO AFSMC.

Acknowledgements

This work is supported by the National Science Council, Taiwan, ROC, under Grants NSC98-2221-E-006-211-MY3 and NSC 98-2221-E-006-212-MY3.

References

[1] R.K. Barai, K. Nonami, Optimal two-degree-of-freedom fuzzy control for locomotion control of a hydraulically actuated hexapod robot, Information Sciences 177 (2007) 1892–1915.
[2] C.-S. Chen, Dynamic structure adaptive neural fuzzy control for MIMO uncertain nonlinear systems, Information Sciences 179 (2009) 2676–2688.
[3] C.-Y. Chen, T.-H.S. Li, Y.-C. Yeh, EP-based kinematic control and adaptive fuzzy sliding-mode dynamic control for wheeled mobile robots, Information Sciences 179 (2009) 180–195.
[4] F. Da, W. Song, Fuzzy neural networks for direct adaptive control, IEEE Transactions Industrial Electronics 11 (6) (2003) 1471–1480.
[5] P.B. Deshpande, R.H. Ash, Computer Process Control with Advanced Control Applications, second ed., Instrument Society of America, North Carolina, 1988.
[6] J. Echanobe, I. del Campo, G. Bosque, An adaptive neuro-fuzzy system for efficient implementations, Information Sciences 178 (2008) 2150–2162.
[7] Y. Feng, X. Yu, Z. Man, Non-singular terminal sliding-mode control of rigid manipulators, Automatica 38 (2002) 2159–2167.
[8] Y. Guo, P.-Y. Woo, An adaptive fuzzy sliding-mode controller for robotic manipulators, IEEE Transactions on Systems, Man, and Cybernetics – Part A: Systems and Humans 33 (2) (2003) 149–159.
[9] H.F. Ho, Y.K. Wong, A.B. Rad, Robust fuzzy tracking control for robotic manipulators, Simulation Modelling Practice and Theory 15 (2007) 801–816.
[10] M.-Y. Hsiao, T.-H.S. Li, J.-Z. Lee, C.-H. Chao, S.-H. Tsai, Design of interval type-2 fuzzy sliding-mode controller, Information Sciences 178 (2008) 1696–1716.
[11] Y.-C. Hsu, G. Chen, H.-X. Li, A fuzzy adaptive variable structure controller with applications to robotic manipulators, IEEE Transactions on Systems, Man, and Cybernetics – Part B: Cybernetics 31 (3) (2001) 331–340.
[12] Y.-J. Huang, T.-C. Kuo, S.-H. Chang, Adaptive sliding-mode control for nonlinear systems with uncertain parameters, IEEE Transactions on Systems, Man, and Cybernetics – Part B: Cybernetics 38 (2) (2008) 534–539.
[13] D. Huang, S.K. Nguang, Static output feedback controller design for fuzzy systems: an ILMI approach, Information Sciences 177 (2007) 3005–3015.
[14] J.Y. Hung, W. Gao, J.C. Huang, Variable structure control: a survey, IEEE Transactions Industrial Electronics 40 (1) (1993) 2–22.
[15] S. Janardhanan, B. Bandyopadhyay, On discretization of continuous-time terminal sliding-mode, IEEE Transactions on Automatic Control 51 (9) (2006) 1532–1536.
[16] T.W. Kim, J. Yuh, Application of on-line neuro-fuzzy controller to AUVs, Information Sciences 145 (2002) 169–182.
[17] C.-L. Kuo, T.-H.S. Li, N.R. Guo, Design of a novel fuzzy sliding-mode control for magnetic ball levitation system, Journal of Intelligent and Robotic Systems 42 (3) (2005) 295–316.
[18] T.-H.S. Li, M.-Y. Hsiao, J.-Z. Lee, S.-H. Tsai, Controlling a time-varying unified chaotic system via interval type 2 fuzzy sliding-mode technique, International Journal of Nonlinear Sciences and Numerical Simulation 10 (2) (2009) 171–180.
[19] T.-H.S. Li, J.-Z. Lee, M.-Y. Hsiao, S.-H. Tsai, Robust interval fuzzy control of a class of uncertain chaotic system, International Journal of Nonlinear Sciences and Numerical Simulation 10 (2) (2009) 81–190.
[20] J.-H. Li, T.-H.S. Li, T.-H. Ou, Design and implementation of fuzzy sliding-mode controller for a wedge balancing system, Journal of Intelligent and Robotic Systems 37 (3) (2003) 285–306.
[21] T.-H.S. Li, K.-J. Lin, Stabilization of singularly perturbed fuzzy systems, IEEE Transactions on Fuzzy Systems 12 (5) (2004) 579–595.
[22] T.-H.S. Li, S.-H. Tsai, M.-Y. Hsiao, Robust fuzzy control for a class of time-delay fuzzy bilinear systems with an additive disturbance, International Journal of Nonlinear Sciences and Numerical Simulation 10 (3) (2009) 315–322.
[23] K.-Y. Lian, C.-H. Su, C.-S. Huang, Performance enhancement for T-S fuzzy control using neural networks, IEEE Transactions on Fuzzy Systems 14 (5) (2006) 619–627.
[24] Y.-W. Liang, S.-D. Xu, D.-C. Liaw, C.-C. Chen, A study of T-S model-based SMC scheme with application to robot control, IEEE Transactions on Industrial Electronics 55 (11) (2008) 3964–3971.
[25] C.-K. Lin, Nonsingular terminal sliding-mode control of robot manipulators using fuzzy wavelet networks, IEEE Transactions on Fuzzy Systems 14 (6) (2006) 849–859.
[26] C.-K. Lin, Robust adaptive critic control of nonlinear systems using fuzzy basis function networks: an LMI approach, Information Sciences 177 (2007) 4934–4946.
[27] Y.-J. Liu, W. Wang, Adaptive fuzzy control for a class of uncertain nonaffine nonlinear systems, Information Sciences 177 (2007) 3901–3917.
[28] I. Lopez-Juarez, J. Corona-Castuera, M. Pena-Cabrera, K. Ordaz-Hernandez, On the design of intelligent robotic agents for assembly, Information Sciences 171 (2005) 377–402.
[29] B. Mansouri, N. Manamanni, K. Guelton, A. Kruszewski, T.M. Guerra, Output feedback LMI tracking control conditions with H_∞ criterion for uncertain and disturbed T-S models, Information Sciences 179 (2009) 446–457.
[30] J.B. Mbede, P. Ele, C.-M. Mveh-Abia, Y. Toure, V. Graefe, S. Ma, Intelligent mobile manipulator navigation using adaptive neuro-fuzzy systems, Information Sciences 171 (2005) 447–474.
[31] W. Pedrycz, Why triangular membership functions, Fuzzy Sets and Systems 64 (1994) 21–30.
[32] W. Pedrycz, Fuzzy equalization in the construction of fuzzy sets, Fuzzy Sets and Systems 119 (2001) 329–335.
[33] W. Pedrycz, F. Gomide, An Introduction to Fuzzy Sets: Analysis and Design, MIT Press, Cambridge, MA, 1998.
[34] W. Pedrycz, J. Valente de Oliveira, A development of fuzzy encoding and decoding through fuzzy clustering, IEEE Transactions on Instrumentation and Measurement 57 (4) (2008) 829–837.
[35] R.-E. Precup, S. Preitl, PI-fuzzy controllers for integral plants to ensure robust stability, Information Sciences 177 (2007) 4410–4429.
[36] E.N. Sanchez, H.M. Becerra, C.M. Velez, Combining fuzzy PID and regulation control for an autonomous mini-helicopter, Information Sciences 177 (2007) 1999–2022.
[37] M. Roopaei, M.Z. Jahromi, Chattering-free fuzzy sliding-mode control in MIMO uncertain systems, Nonlinear Analysis 71 (2009) 4430–4437.
[38] R. Sepu'lveda, O. Castillo, P. Melin, A.R. Dı'az, O. Montiel, Experimental study of intelligent controllers under uncertainty using type-1 and type-2 fuzzy logic, Information Sciences 177 (2007) 2023–2048.
[39] J.J.E. Slotine, W. Li, Applied Nonlinear Control, Prentice-Hall, Englewood Cliffs, NJ, 1991.
[40] M. Sun, S.S. Ge, I.M.Y. Mareels, Adaptive repetitive learning control of robotic manipulators without the requirement for initial repositioning, IEEE Transactions on Robotics 22 (3) (2006) 563–568.
[41] C.W. Tao, J.S. Taur, M.-L. Chan, Adaptive fuzzy terminal sliding-mode controller for linear systems with mismatched time-varying uncertainties, IEEE Transactions on Systems, Man, and Cybernetics – Part B: Cybernetics 34 (1) (2004) 255–262.
[42] C.-S. Ting, An observer-based approach to controlling time-delay chaotic systems via Takagi–Sugeno fuzzy model, Information Sciences 177 (2007) 4314–4328.
[43] S. Tong, Y. Li, P. Shi, Fuzzy adaptive backstepping robust control for SISO nonlinear system with dynamic uncertainties, Information Sciences 179 (2009) 1319–1332.

[44] L. Wang, T. Chai, L. Zhai, Neural-network-based terminal sliding-mode control of robotic manipulators including actuator dynamics, IEEE Transactions on Industrial Electronics 56 (9) (2009) 3296–3304.
[45] L.K. Wong, F.H.F. Leung, P.K.S. Tam, A fuzzy sliding controller for nonlinear systems, IEEE Transactions on Industrial Electronics 48 (1) (2001) 32–37.
[46] N. Yagiz, Y. Hacioglu, Y. Taskin, Fuzzy sliding-mode control of active suspensions, IEEE Transactions on Industrial Electronics 55 (11) (2008) 3883–3890.
[47] J. Yoneyama, Robust stability and stabilizing controller design of fuzzy systems with discrete and distributed delays, Information Sciences 178 (2008) 1935–1947.
[48] S.-J. Yoo, J.-B. Park, Y.-H. Choi, Adaptive dynamic surface control of flexible-joint robots using self-recurrent wavelet neural networks, IEEE Transactions on Systems, Man, and Cybernetics – Part B: Cybernetics 36 (6) (2006) 1342–1355.
[49] X.H. Yu, M. Zhihong, Fast terminal sliding-mode control design for nonlinear dynamical systems, IEEE Transactions on Circuits and Systems I: Fundamental Theory and Applications 49 (2) (2002) 261–264.
[50] L.A. Zadeh, Toward a generalized theory of uncertainty (GTU) – an outline, Information Sciences 172 (2005) 1–40.
[51] L.A. Zadeh, Is there a need for fuzzy logic, Information Sciences 178 (2008) 2751–2779.
[52] M. Zhihong, A.P. Paplinski, H.R. Wu, A robust MIMO terminal sliding-mode control scheme for rigid robotic manipulators, IEEE Transactions on Automatic Control 39 (12) (1994) 2464–2469.
[53] M. Zhihong, X.H. Yu, Terminal sliding-mode control of MIMO linear systems, IEEE Transactions on Circuits and Systems I 44 (11) (1997) 1065–1070.